Desalination and Water Treatment
www.deswater.com
doi: 10.5004/dwt.2022.28043

247 (2022) 17–27
January

Synthesis of nanocomposite membranes embedded with cellulose nanocrystals and their application to filtrate of arsenic aqueous solutions

Milad Hashemibeni[a], Elham Ameri[a,*], Javad Hashemibeni[b], Hesam Seifi[a]

[a]*Department of Chemical Engineering, Shahreza Branch, Islamic Azad University, P.O. Box: 311-86145, Shahreza, Iran, Tel. +98 321 3292242; Fax: +98 265 2423898; emails: ameri@iaush.ac.ir (E. Ameri); miladhashemi1991@yahoo.com (M. Hashemibeni), hesam.saifi55@yahoo.com (H. Seifi)*
[b]*Department of Mechanical and Electrical Engineering, University of Electronic Science and Technology of China, Chengdu, Sichuan, China, email: javad.hashemi1987@yahoo.com*

Received 21 June 2021; Accepted 11 December 2021

ABSTRACT

The present study focused on the performance enhancement of thin-film nanocomposite membranes by incorporation of cellulose nanocrystals to remove arsenic from water in the nanofiltration process. The nanofiltration membranes were fabricated by interfacial polymerization. The fabricated membranes were prepared by the addition of different amounts of cellulose nanocrystals (CNC) at concentrations of 0%, 0.1%, 0.5% and 1 wt.% coded NF0, NF0.1, NF0.5 and NF1, respectively. The properties of the membranes were investigated by attenuated total reflectance-Fourier-transform infrared spectroscopy, scanning electronic microscopy, and water contact angle test. The results showed that after 200 min, the water flux through the NF0 and NF1 membranes was approximately 260 and 148 L/m^2 h, respectively. Results also showed that the anti-sediment property was improved with the increasing CNC content of the membranes, by increasing the hydrophilicity of the membrane surface or negative surface charge of CNC. The maximum percentage of arsenic removal of 96.45% was achieved for the feed mixture at an initial arsenic concentration of 5 mg/L, using NF0.5 membrane for 45 min.

Keywords: Membrane; Nanofiltration; Nanocomposite; Cellulose nanocrystal; Arsenic

1. Introduction

With the growth of urbanization and the rapid industrialization of cities, the problem of the release of heavy metals into the ecosystem, even in small concentrations, has raised concerns in many parts of the world. There are strict laws in many countries because of the presence of heavy metals in water and sewage to control water pollution [1]. Arsenic is a very toxic semi-metal for humans, animals and many plants [2]. Despite their toxic effect, inorganic arsenic bonds occur on earth naturally in small amounts. Humans may be exposed to arsenic through food, water and air. Exposure may also occur through skin contact with soil or water that contains arsenic. High levels of this material in the human body are causing skin, lung and bladder cancers [3–5]. Many parts of the world are contaminated with this material because arsenic is naturally present in water and soil and is also produced by human activities such as agriculture and mining [6]. The World Health Organization (WHO) and many international legislatures have proposed a maximum concentration of

* Corresponding author.

0.01 mg/L of arsenic in water to protect against the toxicity of this substance [7]. Membrane manufacturing processes to be paid attention to due to the advantages such as reducing the energy required for separation and the possibility of achieving high decontamination coefficient, more selectivity compared to other separation methods without the need for special additives, and low cost in wastewater treatment processes containing heavy metals. Membrane filtration techniques have simple utilization, low energy cost, and high efficiency [8]. In this regard, the removal of arsenic ions from their aqueous solution using membrane processes such as nano-filtration and reverse osmosis was extensively studied. In 2010, arsenic removal from drinking water using a thin-film composite (TFC) nanofiltration membrane was investigated. The results of this study showed that the removal of arsenate ions by TFC membranes with total dissolved solids and other contaminants was found to be 99.8%. High flux at the end of each experiment with TFC membrane at a working time of 180 min indicated that the membranes were not affected by the fouling during the process [9]. In 2012, the effectiveness of a reverse osmosis system in removing arsenic from drinking water was studied. The results showed that the parameters of concentration, pH, solution temperature and pressure affected the performance of reverse osmosis membranes and increasing or decreasing of parameters led to change in their efficiency and performance [10]. In 2013, a study investigated the fabrication and characterization of a new membrane of the PES/Fe-Mn dual oxidation ultrafiltration matrix to remove (III) from contaminated water solution. The best membrane performance was achieved by using the membrane prepared with FMBO/PES ratio of 1.5: 1. The water flux of up to 94.6 L/m^2 h at an operating pressure of 1 bar, and maximum absorption of As(III) of about 73 mg/g were resulted [11]. In 2014, the performance of polyamide nanofiltration in comparison with low-pressure reverse osmosis membranes in the removal of trivalent arsenic under different operating conditions was studied. It was found that the arsenic removal was significantly increased with increasing pH. Also, the removal efficiencies for TFC and low-pressure reverse osmosis membranes were found to be 40% and 90%, respectively [12]. In 2015, a study evaluated the efficiency of a reverse osmosis system in the removal of heavy metal arsenic from drinking water at different system conditions (pressure, temperature and pH). The results showed that with increasing pressure, the percentage of arsenic removal and the average output flux of the membranes increase [13]. In 2019, a study examined cellulose polyamide nanofiltration membranes with cellulose nanocrystals to increase water flux and chlorine resistance. Cellulose nanocrystals (CNCs) were prepared by hydrolysis of sulfuric acid. Microcrystalline cellulose was fabricated directly in aqueous piperazine solution to make thin-film nanocomposite membranes by interfacial polymerization. These membranes, in comparison with thin-film non-CNC composite membranes, were more hydrophilic and they had more porous surfaces, thus they increased the water infiltration flux. Eliminating of Na_2SO_4 and $MgSO_4$ salts from their solutions were obtained 98.3% and 96.1%, respectively [14]. In 2020, the effect of the surface charges of thin-film composite membranes for the removal of copper(II) ions using nanofiltration and direct osmosis was investigated. Membranes with a 1PIP/1PEI ratio show the highest copper(II) ion removal rate more than 95% and 99% in nanofiltration and direct osmosis processes, respectively [15]. Reviewing literature shows that the thin-film composite membranes showed great results for heavy metal removal. Also, membranes with the integration of nano-particles into the polymer matrix were investigated to remove heavy metals from their wastewaters. In 2012, a new membrane of polyethersulfone nanocomposite prepared with PANI/Fe_3O_4 nanoparticles with high performance for Cu(II) removal was investigated. The results showed that the membrane with the presence of 0.1% nanoparticles had the highest rate of Cu ion removal, but the lowest pure water flux [16]. In 2020, the incorporation of CNC into polyamide thin-film composite membranes was investigated in a nanofiltration process. The water flux was significantly increased (more than 23%) while maintaining high rejection rate values for sodium chloride (98.3% ± 0.8%) and calcium chloride (97.1% ± 0.5%). Furthermore, there was also an increase in the thermal stability of the membrane [17]. Also, cellulose nanocrystal/silver (CNC/Ag) thin-film nano-composite nanofiltration membranes with multifunctional properties were investigated. The incorporation of 0.01 wt.% CNC/Ag into the nano-composites led to achieving high pure water permeability and high rejection rate of Na_2SO_4 (99.1%). Besides, the membrane also exhibited exceptional antifouling (flux recovery ratio reaches 92.6% for humic acid) and antibacterial performance (99.4% reduction of *Escherichia coli* viability) [18]. In 2019, a nanocomposite membrane for reverse osmosis applications was investigated. Desalination experiments with synthetic brackish water revealed a doubling of the water flux from 30 to 63 ± 10 L/m^2 h, for 0.1% (w/v) CNCs loading [19]. Polyethersulfone/modified cellulose nanocrystals nanocomposite membranes were used for industrial wastewater treatment. The results showed that the nanocomposite membranes at 1 wt.% CNC concentration had the best efficiency of color removal from industrial wastewater [20]. More recently, improvement of filtration and antifouling performance of cellulose acetate membrane reinforced by dopamine modified CNC properties was investigated. These membranes showed a broad application prospect in the field of biological separation membrane and water treatment membrane [21]. In 2021, the effect of carboxylated cellulose nanocrystals integration in the performance of thin-film composite membrane was investigated. The enhancement of the mechanical properties of the membrane was due to the compatibility between CNCs and the polyethersulfone ultrafiltration support [22].

In this research, we try to fabricate and study the properties of nanocomposite membranes modified with cellulose nanocrystals in the process of removing arsenic from water. The prepared membranes were identified by various detection techniques such as attenuated total reflectance-Fourier-transform infrared spectroscopy (ATR-FTIR), scanning electronic microscopy (SEM), and water contact angle test. Then, these nanofiltration membranes modified with cellulose nanocrystals were used to remove arsenic from aqueous media.

2. Materials and methods

2.1. Material

Udel P-2700 polysulfone polymer was purchased from Solvay Advanced Polymers Co., 1-methyl-2-pyrrolidone (NMP > 95%) and polyvinylpyrrolidone (PVP > 97%) with the molecular weight of 40,000 g mol^{-1} were obtained by Sigma-Aldrich, trimesoyl chloride (TMC, 99 piperazine (PIP, 99%) and hexane (99%) were obtained from Merck Co. Cellulose nanocrystals (CNC) (purity more than 95%) with dimensions less than 40 nm was prepared by Sigma-Aldrich. Sodium arsenate salt ($Na_2HA_SO_4$, $7H_2O$) was obtained from Merck Company to prepare the arsenic solutions with different concentrations. Also, sodium hydroxide (NaOH) and hydrochloric acid (HCl) with 99% purity from Merck Company were used to regulate the alkaline and acidic environment of the aqueous solution.

2.2. Preparation of nanofiltration membranes

First, a certain amount of NMP solvent (82 wt.%) was added into a beaker then a certain amount of PVP (0.5 wt.%) was added and mixed with a magnetic stirrer then placed on a magnetic stirrer and slowly polysulfone (17.5 wt.%) was added (add slowly to prevent sticking) and placed on the mixer at room temperature for 24 h until completely dissolved then placed in a stationary place to remove the bubbles from the solution step by step. The solution was then poured onto a 2 mm thick glass plate using a molding film and rapidly placed in an aqueous coagulation bath at room temperature to cause a phase inversion to separate the membrane from the glass plate. Then, it was transferred to another water bath to remove any remaining material and water particles. Finally, it was put into the water for a few hours and then put polyamide layers on it [23]. TMC organic solution in hexane with a concentration of 0.15% was prepared after 24 h under magnetic stirring. Different concentrations (0.1, 0.5 and 1 wt.%) of CNC were added to the TMC organic solution and irradiated with an ultrasonic bath for 1 h. Aqueous PIP solution in water with a concentration of 2% was prepared after 24 h under magnetic stirring. Place the substrate (polysulfone) on the frame and add 20 cc of PIP aqueous solution to be completely immersed in the solution. Remove the excess solution after 2 min and smoothed with rollers. 20 cc of TMC organic solution with a specified concentration of CNC solution was added to the frame, the remaining solution was evacuated for 1 min and the membranes were placed in an oven at 90°C for 10 min to dry. After drying, the membranes are immersed in pure ethanol for 3 min [23]. PSF membranes were named NF0, NF0.1, NF0.5 and NF1 based on different concentrations of nanocrystals.

2.3. Determination of membranes properties

ATR-FTIR spectrometer (Model UATR, Perkin-Elmer US) was used to ensure the chemical structure of the membranes. Spectra were performed in the range of CM-1500-4000. The nanofiltration membranes were dried for 60 h at 60°C and then tested by FTIR. The morphology of the membranes was evaluated using field scanning electron microscopy of Shimadzu, Hitachi, Japan.

In these experiments, an angle detector (optical contact angle measuring device OCA15plus, Germany, DATA Physics) was used and the angle of water droplets with the membranes surfaces was measured. To minimize the measurement error, the contact angle was examined at 10 points from the membranes surfaces and their mean was reported as the contact angle with water. ATR-FTIR spectrometer (Model UATR, Perkin-Elmer US) was used to ensure the chemical structure of the membranes. Spectra were performed in the range of CM 1500-4000. The nanofiltration membranes were dried at 60°C, for 60 h, and then tested by FTIR. The morphology of the membranes was evaluated using field scanning electron microscopy of Shimadzu, Hitachi, Japan.

In these experiments, an angle detector (optical contact angle measuring device OCA15plus, Germany, DATA Physics) was used and the angle of water droplets with the membranes surfaces was measured to minimize the measurement error, the contact angle was examined at 10 points from the membranes surfaces and their average of results were reported as the contact angle with water.

2.4. Evaluation of nanofiltration membrane performance

Fig. 1 shows the nanofiltration system for evaluating the performance of nanofiltration membranes. This system includes a feeding tank, tank outlet valve, fluid transferring pump, return flow valve, flowmeter, barometer, membrane cell and feeding tank inlet valve. The membrane areas were 14.62 cm^2. The nanofiltration process was performed under operating conditions, pressure 6 bar, the flow rate of 2 L/min and ambient temperature.

The performance of the membranes to remove arsenic from the water was measured by a nanofiltration system. First, the stock solution of 200 mg/L arsenic was prepared by dissolving sodium arsenate (Na_2HASO_4, $7H_2O$) in HPLC grade distilled water. Then concentrations of 5, 10, 15, 20, 40 and 80 mg/L were made from the stock solution. The pH of the aqueous cadmium solution was also adjusted between 3 and 10. For adjusting the pH of the solutions, the solutions of 0.1 M NaOH and 0.1 M HCl were used. Pure water was passed through the nanofiltration membranes for 60 min and the flow rate was measured. The solution containing arsenic salts was replaced with pure water. The schematic diagram of the principle of the membrane separation of arsenic ions is given in Fig. 1b. The separation was performed based on the molecular size of the water and that of the arsenic ions. The small size of the water molecules compared to the arsenic ions causes to diffusing the water molecules through the nanofiltration membrane pores, while the arsenic ions due to their large size could not diffuse through the membrane.

The passage test of sodium arsenate salt solution (Na_2HASO_4, $7H_2O$) was performed under different conditions. The concentration of arsenic heavy metal in the penetrant phase was measured by an atomic absorption spectrometer. Therefore, Eqs. (1) and (2) should be used to obtain the water flux through the nanofiltration membranes [21].

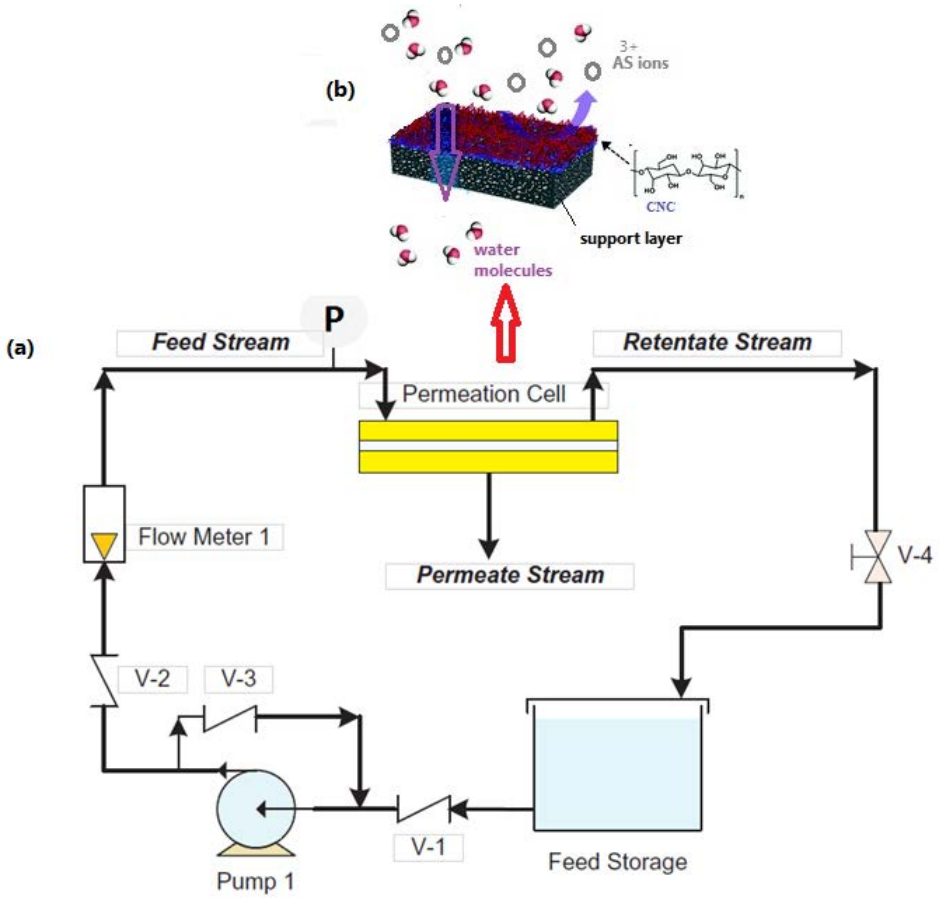

Fig. 1. Nanofiltration system to evaluate the performance of membranes.

$$J = \frac{\Delta V}{A_m \cdot \Delta t} \tag{1}$$

$$A = \frac{J}{\Delta P} \tag{2}$$

where A_m is the effective area of the membranes, ΔV is the volume of passing water through the membranes, Δt is the time difference and ΔP is the pressure difference. Eq. (3) is also used for the amount of heavy metal rejection [24].

$$R = \left(1 - \frac{C_p}{C_f}\right) \times 100 \tag{3}$$

where C_p and C_f are the concentration of penetrated heavy metals, and the concentration of heavy metals in the feeding section, respectively.

2.5. Fouling and antifouling tests

The fouling of the fabricated nanofiltration membranes were evaluated for 8 h at room temperature and at 8 bar. The fouling of the membranes depends on the hydrodynamic performance conditions and the composition of the inlet feed to the nanofiltration system. Therefore, a solution of 10 mM sodium chloride and 200 mg/L BSA in distilled water were prepared and used as a feed solution. In this solution, BSA acts as a plasticizer. We facilitated the sedimentation process with a feed flow rate of 1.4 L/min. After 8 h, the water flux recovery test was performed by cleaning the membranes. Therefore, distilled water instead of NaCl/BSA feed solution was circulated in all membranes area at a speed of 1.4 L/min for 60 min without applying pressure to the membranes. Then the operating passed water flux similar to the NF0 process was measured.

3. Results and discussion

3.1. FTIR spectrometry analysis

Fig. 2 shows the FTIR spectrum of a pure membrane and a nanocomposite membrane in the presence of CNC. 1,150 cm^{-1} peaks are related to the symmetrical stretching bonds O=S=O and 1,300 cm^{-1} peaks are related to the asymmetric stretching bonds O=S=O and 1,530 cm^{-1} peaks are related to the C=C aromatic ring stretching bonds due to PSF polymer groups [25]. The peak at 1,623 cm^{-1} assigned to C=O band of the amide group is observed in both membranes indicating that polymerization took place [26].

The region observed at 3,100–3,400 cm^{-1} was related to the N–H stretching bands of amide, and the peak at 1,582 cm^{-1} was pointed to the N–H bending bond of that.

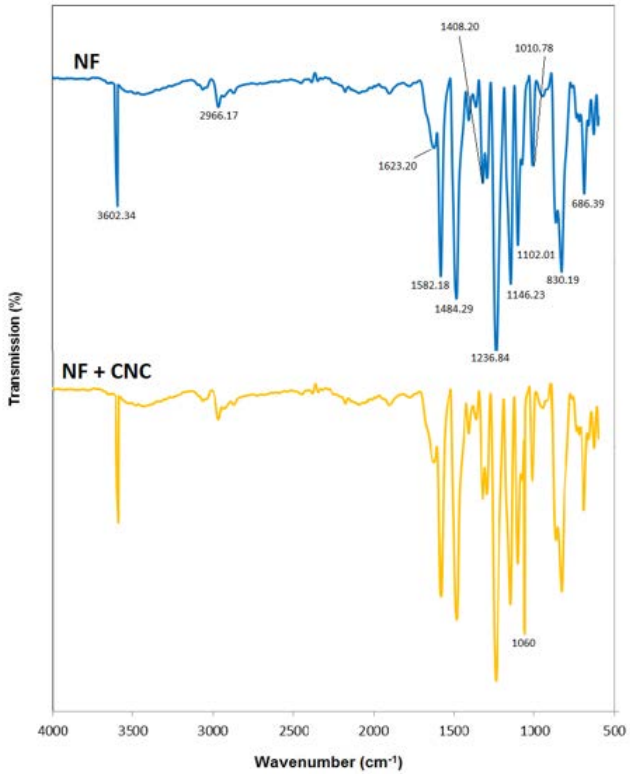

Fig. 2. FTIR spectrum of NF0 membrane and NF0.1 membranes.

The peak at 3,500 cm^{-1} indicated the presence of hydroxyl groups of the CNC. The peak of 2,902 cm^{-1} is related to the symmetric stretching vibrations of C–H bonds [27]. The peaks of 1,643 and 1,431 cm^{-1} are related to the O–H stretching vibration bonds, which are related to water absorption and the $–CH_2$ stretching vibration bonds. The peak of 1,075 cm^{-1} on C–O–C stretching vibrations bonds was related to the cellulose bond and confirmed the presence of cellulose nanocrystals in the membrane [28].

3.2. Energy-dispersive X-ray analysis

The results of energy-dispersive X-ray analysis (EDX) are shown in Table 1. The EDX spectrum of the unmodified membranes represented three peaks around the binding energies with the atoms of carbon (C), oxygen (O), and sulfur (S). Since cellulose nanoparticles are composed of the same elements, the analysis of the spectra of polysulfone nanocomposite membranes and cellulose nanoparticles showed different percentages of these elements.

3.3. Morphology of the prepared membranes

The prepared nano-composite and pure membranes were morphologically characterized using SEM. SEM micrographs of the cross-section of the samples showed the pores through the membranes. The distribution of CNC was quite uniform in membranes with 0, 0.1, and 0.5 wt.% and the polymer-filler interface was of good quality. As shown in Fig. 3, CNC agglomeration at the polymer filler interface was observed in the membrane incorporating CNC upper than 0.5%. CNC agglomeration causes the demolition of polyamide membrane layer uniformity and hence defects in the layer. These defects might cause the heavy metal molecules to pass through the membranes resulting in a reduction of membrane selectivity [29]. Also, the accumulation of these nano-crystals on the membranes surfaces causes blockage of membranes pores and reduces the rate of penetration into the membranes [25].

Table 1
Results of energy dispersive X-ray analysis

Membrane	Element (wt.%)			Total
	C	O	S	
NF	80.77	15.95	2.95	100
NF0.1	81.21	15.69	3.1	100

3.4. Contact angle test

Contact angle values of upper layers of the membranes were measured and the results are presented in Fig. 4. By adding nanocellulous with different concentrations to the surfaces of nanocomposite membranes, the contact angle of the membranes surfaces with water was reduced.

Reducing the contact angle with water means, increased the hydrophilicity of the nanocomposite membranes. The reason for increasing the hydrophilicity of nanocomposite membranes is the presence of CNC hydrophilic nanoparticles on the upper surfaces and membranes structure [30].

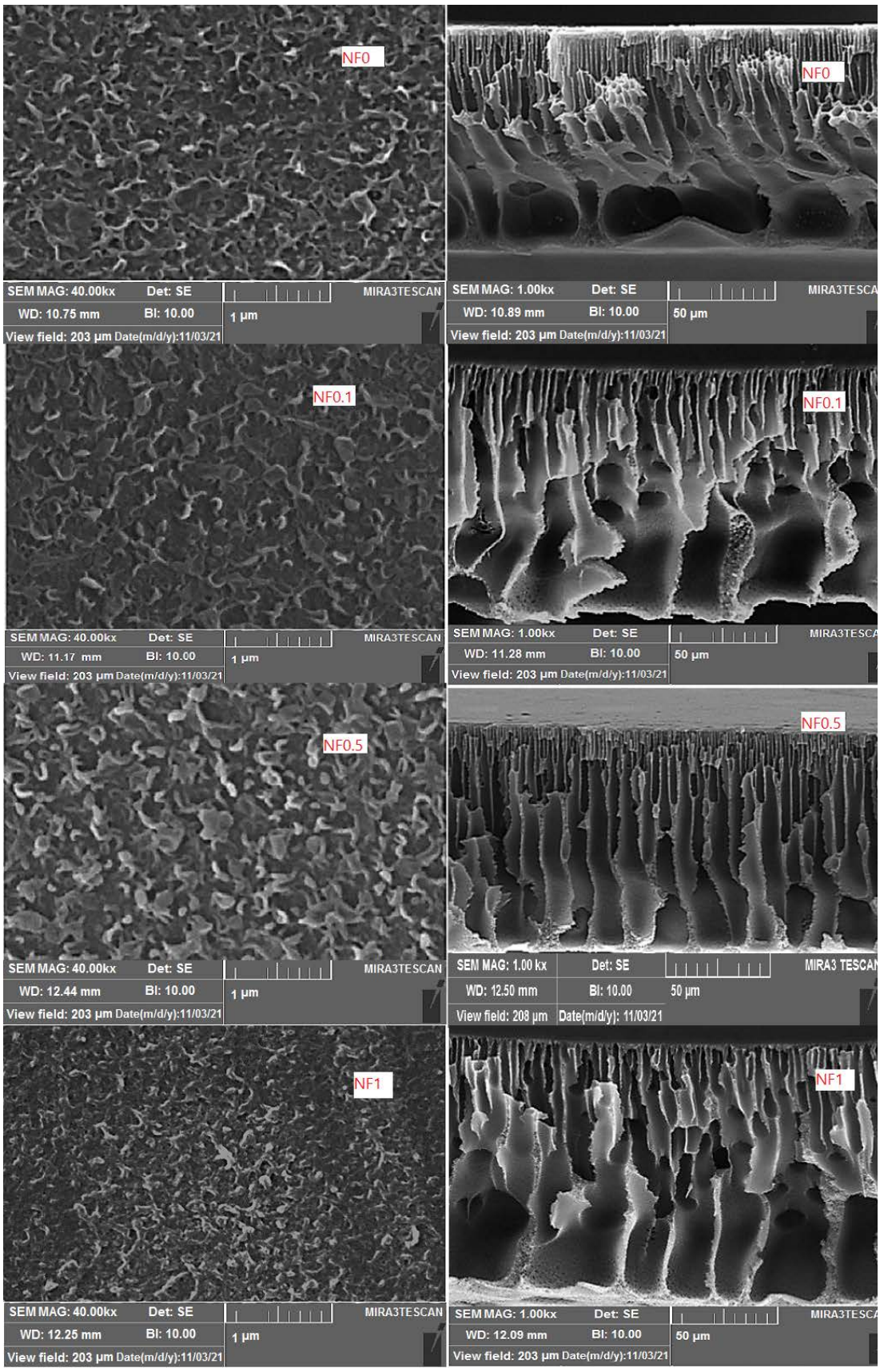

Fig. 3. SEM images of upper surface and cross-section of membranes, (a) NF0, (b) NF0.1, (c) NF0.5 and (d) NF1 membranes.

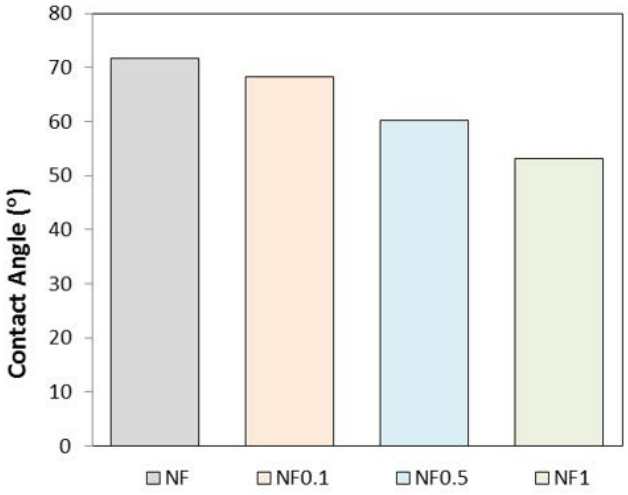

Fig. 4. Contact angle between water and membranes.

As shown in Fig. 4, the contact angle of water with the membranes without the presence of CNC was 72.4°, which was reduced to 53.2° by adding 1% CNC.

3.5. Results of water flux through nanofiltration membranes

Fig. 5 shows the water flux through nanofiltration membranes over time. The results show that the incorporation of CNC enhanced the pure water flux through the membrane. This can be due to the presence of hydrophilic cellulose nanocrystals with different concentrations on the surfaces of the pure membranes (NF). Therefore, the presence of cellulose nanocrystals can cause more hydrophilicity and increase wettability of the membranes.

As shown in Fig. 5, the water flux of the pure water through the membranes was initially decreased with increasing time and after a while was almost constant. The reason for this observation could be refer to the membrane compaction and non-uniform polyamide layer formed on the PSf support. In addition, the presence of the arsenic ions in the feed solution initially decreased the water flux, due to the placement of ions in some pores in the membrane surface. After that the repulsion forces generated between the adsorbed ions onto the membrane surface and these ions in the feed solution led to a decrease in the membrane fouling rate and, therefore, the water flux remains constant. At the end of the nanofiltration process and after 200 min, the water flux through the NF0 membranes was approximately 260 L/m^2 h and the water flux through the NF1 membrane was 148 L/m^2 h.

3.6. Arsenic removal results using nanofiltration membranes

3.6.1. pH effect

The effect of pH of the solution on the rate of arsenic removal by nanofiltration membranes was investigated under operating conditions of the pressure of 6 bar, flow rate of 2 L/min, initial concentration of arsenic 5 mg/L, and during 60 min at 25°C. As shown in Fig. 6 arsenic removal with different membranes was increased with increasing

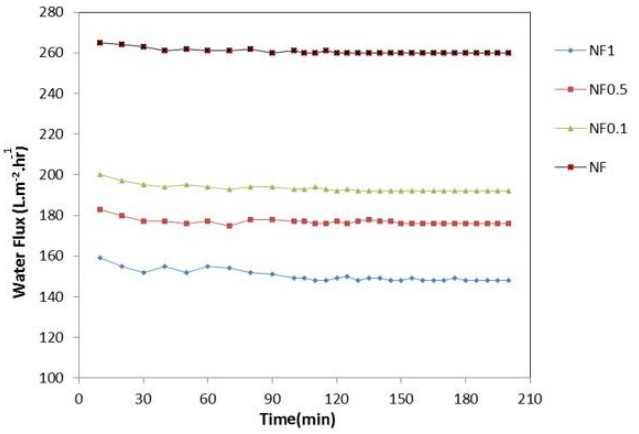

Fig. 5. Water flux of pure water through nanofiltration membranes vs. test time.

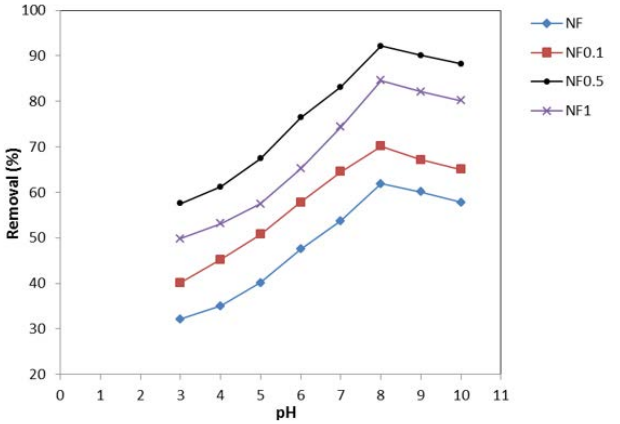

Fig. 6. Effect of pH on the percentage of arsenic removal in different membranes under different operating conditions (pressure 6 bar, flow rate 2 L/min, initial arsenic concentration 5 mg/L, time 60 min and temperature 25°C).

pH from 2% to 8%. With further enhancement of pH from 8 to 10, the amount of arsenic removal was decreased with a low slope.

At pHs up to 8, the OH-environment ions was increased and this led to their competition with the membranes in the adsorption of arsenic ions. Therefore, the adsorption of arsenic ions by the membranes was decreased. In the alkaline range above 8, membrane fouling plays an important role in the removal of arsenic ions [31]. The highest percentage of arsenic removal achieved at pH 8. These amounts for NF0 and NF1 membranes were 61.92% and 92.14%, respectively. In other study, nanofiltration membranes were used to remove arsenic, and the percentage of arsenic removal was 85% at pH 8.5 [32].

3.6.2. Cellulose nanocrystal concentration effect

Fig. 7 shows the percentage of arsenic removal using nanocomposite membranes with different contents of CNC under operating conditions of a pressure of 8 bar, the flow rate of 2 L/min, pH 8, initial concentration of arsenic

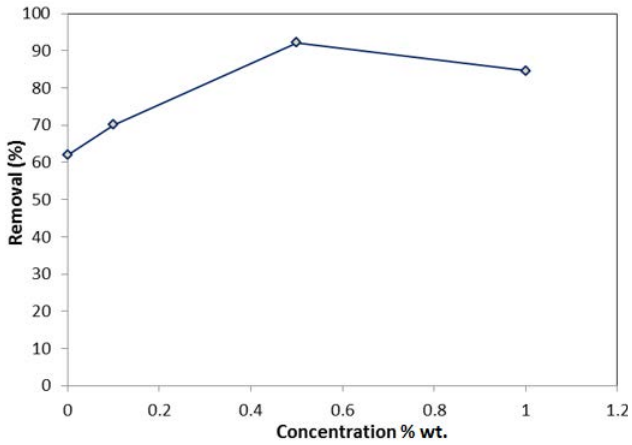

Fig. 7. Percentage of arsenic removal in nanocomposite membranes with different concentrations of CNC under operating conditions (pressure 8 bar, flow 2 L/min, pH 8, initial concentration of cadmium 80 mg/L, time 60 min and temperature 25°C.

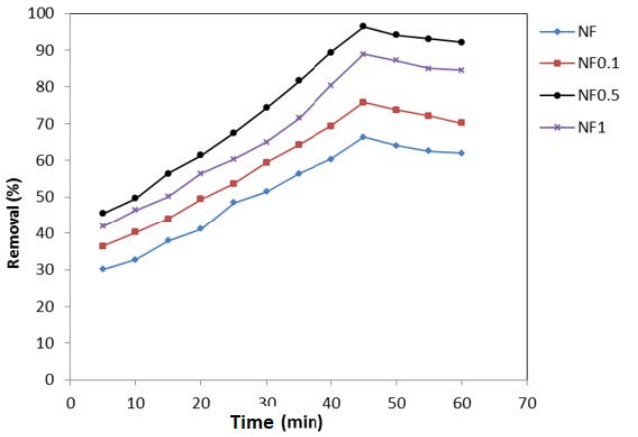

Fig. 8. Removal percentage of arsenic over time by different nanofiltration membranes. (Operating conditions: 6 bar pressure, flow 2 L/min, pH 8, initial concentration of arsenic 5 mg/L and temperature 25°C).

80 mg/L during 60 min at 25°C. As can be seen, adding CNC to the surface of nanofiltration membranes had a positive effect on their adsorption. This is a very common phenomenon and is observed for all inorganic nanoparticles. Nanofiltration membranes with CNC have good adsorption, and this high ability was increased for nanocellulose membranes with a concentration of 0.5 wt.% (NF0.5), and the percentage of arsenic removal was achieved approximately 93%. The addition of cellulose nanoparticles covers the surface cavities of the membranes. Transmission of the cadmium through the small cavities are difficult, therefore membranes with higher nanocelloluse have stronger adsorption. In other study, the percentage of arsenic removal was obtained above 95%, by using NF0 membranes at relatively low pressure (1.1 MPa) [33].

3.6.3. Time effect

Fig. 8 shows the percentage of arsenic removal at different times using different membranes under operating conditions of pH 8 (optimal), pressure of 8 bar, flow rate of 2 L/min, initial concentration of arsenic 5 mg/L and temperature of 25°C.

As can be seen, the percentage of arsenic removal in different membranes was increased with the time of operation. In NF0.5 membrane because of the presence of CNC, the percentage of arsenic removal was more than other membranes. The percentage of arsenic removal over a period of more than 45 min has a decreasing trend with a slow slope. The highest percentage of arsenic removal was 96.45 during 45 min for NF0.5 membrane.

3.6.4. Initial concentration effect

Fig. 9 shows the percentage of arsenic removal at different initial concentrations of arsenic in different nanofiltration membranes under operating conditions of pH 8, pressure of 8 bar, flow rate of 2 L/min, during 45 min and temperature of 25°C. As can be seen, with increasing the

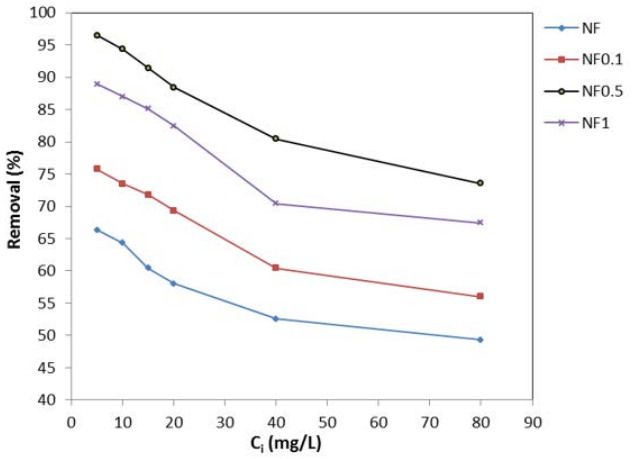

Fig. 9. Percentage of arsenic removal in different initial concentrations of arsenic and in different nanofiltration membranes. Operating conditions: pressure 8 bar, flow 2 L/min, pH 8, time 45 min and temperature 25°C.

initial concentration of arsenic solution for all nanofiltration membranes, the percentage of arsenic removal was decreased.

The highest percentage of arsenic removal by membranes was obtained at an initial concentration of 5 mg/L. In these experiments, the highest percentage of arsenic removal was found to be 96.45% in the initial concentration of 5 mg/L with NF0.5 membrane and the lowest percentage of arsenic removal was found to be 49.33% in the initial concentration of 80 mg/L, with NF0 membrane.

3.7. Membrane fouling studies

Fig. 10 shows the membrane fouling dependence of NF0 and NF0.5 membranes in the nanofiltration process over time. As can be seen, the decreasing of NF0 membrane water flux was more severe than NF0.5 membrane,

Table 2
Comparison between the rates of arsenic removal with different membranes

Adsorbent	pH	Time (min)	Rejection (%)	Flux (L/m² h)	References
NF0.5	8	45	96.45	178	This study
PVDF/FeOOH	9	720	90	–	[38]
PVDF/Zirconia	9	2,880	92	177.6	[39]
Fe_3O_4@AAO	6	40	94	–	[40]
PSF/HINM	7	480	90	87.84	[41]
PPESK	5	60	85	–	[42]
NF	7	60	96	–	[43]
Composite polyamide	8	480	96	–	[44]

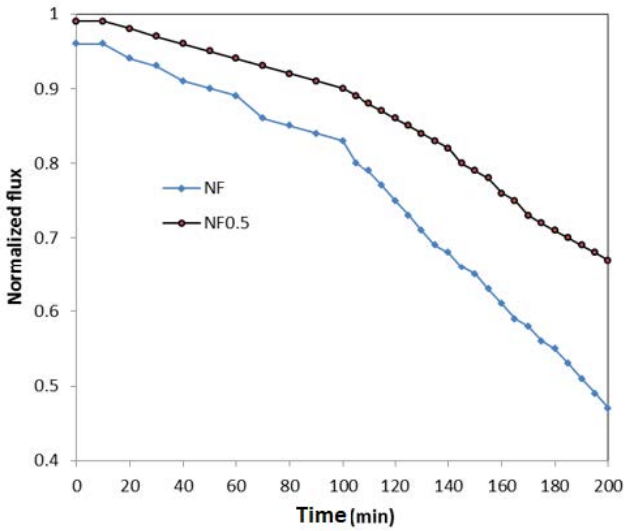

Fig. 10. Organic fouling of NF0 and NF0.5 membranes.

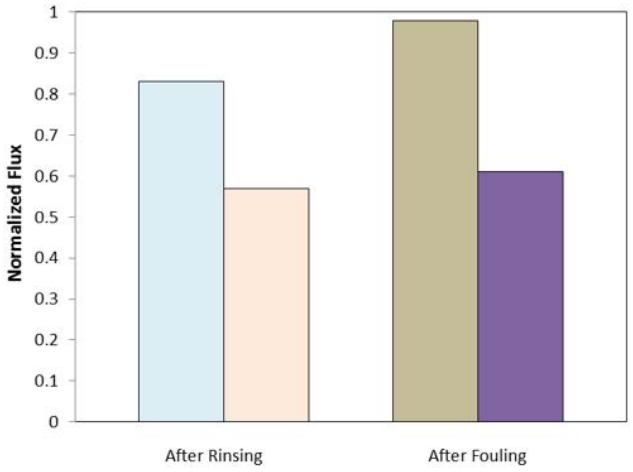

Fig. 11. Comparison of normal flux recovery of NF0 and NF0.5 membranes after washing.

which indicated that NF0.5 membrane was more resistance than NF0 membrane vs. fouling phenomena. The decrease in water flux can be attributed to the formation of a BSA layer on the membranes surfaces. This layer increases the resistance of the membranes to water flux [34].

Addition of CNC to the nanofiltration membranes layers reduced the accumulation of BSA on the NF0.5 membranes surface, which resulted in improved NF0.5 membrane resistances to the membrane fouling [35]. Therefore, increasing the anti-fouling properties of NF0.5 membrane can be obtained by increasing the hydrophilicity of NF0.5 membranes surfaces or negative surfaces charges of CNC [36].

Fig. 11 shows a comparison of the normal fluxes of NF0 and NF0.5 membranes before and after water washing. As shown in Fig. 11, the NF0.5 membranes can obtain about 20.85% of the water flux compared to 6.7% in NF0 membranes, indicating the higher performance of the NF0.5 membrane in improving the water flux through the membrane.

The improved hydrophilicity of NF0.5 weakened the interaction between membrane and BSA, therefore, BSA was easier removed from membrane surface [37].

3.8. Comparison of some reported membranes for arsenic removal

Various membranes have been used to remove arsenic from aqueous solution. Table 2 summarizes the comparison between the rates of arsenic removal with different membranes. Obviously, the membrane proposed (NF0.5) in this study has an extremely high removal capability compared to other membranes reported.

4. Conclusion

The results of this study showed that the flow rate (water flux) of pure water through nanofiltration membranes was initially decreased with increasing time and after a time was almost constant. With increasing pH from 2 to 8, percentage of the arsenic removal with different membranes was increased. With further increases of pH from 8 to 10, the percentage of arsenic removal was decreased with a low slope. The highest percentage of arsenic removal was found to be 92.14% using NF0 membrane, at pH 8. The percentage of arsenic removal over a period of more than 45 min has a decreasing trend with a slow slope. The highest percentage of arsenic removal was 96.45% during 45 min for NF0.5 membrane. With increasing the initial concentration of arsenic solution for all of

the nanofiltration membranes, the percentage of arsenic removal was decreased. The highest percentage of arsenic removal was obtained at an initial concentration of 5 mg/L. Result indicated that NF0.5 membrane was more effective than NF0 membrane in improving the water flux through the nanofiltration process.

Conflict of interest

The authors declare that they have no conflict of interest.

References

[1] B.M.W.P.K. Amarasinghe, R.A. Williams, Tea waste as a low cost adsorbent for the removal of Cu and Pb from wastewater, Chem. Eng. J., 132 (2007) 299–309.

[2] M.I. Litter, Prospect of Rural Latin American Communities for Application of Low-cost Technologies for Water Potabilization OAS Project AE141/2001, Digital Grafic, La Plata, Argentina, 2002.

[3] C.-H. Tseng, C.-K. Chong, C.-P. Tseng, J.A. Centeno, Blackfoot disease in Taiwan: its link with inorganic arsenic exposure from drinking water, Ambio, 36 (2007) 82–84.

[4] Y. Chen, M.E. Hakim, F. Parvez, T. Islam, A.M. Rahman, H. Ahsan, Arsenic exposure from drinking-water and carotid artery intima-medial thickness in healthy young adults in Bangladesh, J. Health Popul. Nutr., 24 (2006) 253–257.

[5] C. Hopenhayn, Arsenic in drinking water: impact on human health, Elements, 2 (2006) 103–107.

[6] Z. Lin, R.W. Puls, Adsorption, desorption and oxidation of arsenic affected by clay minerals and aging process, Environ. Geol., 39 (2000) 753–759.

[7] WHO, Water, Sanitation, and World Health Organization, Guidelines for Drinking-Water Quality, Vol. 1, Rec. 2004.

[8] M. Ghorbani, M.H. Vakili, E. Ameri, Fabrication and evaluation of a biopolymer-based nanocomposite membrane for oily wastewater treatment, Mater. Today Commun., 28 (2021) 102560, doi: 10.1016/j.mtcomm.2021.102560.

[9] R.S. Harisha, K.M. Hosamani, R.S. Keri, S.K. Nataraj, T.M. Aminabhavi, Arsenic removal from drinking water using thin-film composite nanofiltration membrane, Desalination, 252 (2010) 75–80.

[10] P. Daraei, S.S. Madaeni, N. Ghaemi, E. Salehi, M.A. Khadivi, R. Moradian, B. Astinchap, Novel polyethersulfone nanocomposite membrane prepared by PANI/Fe_3O_4 nanoparticles with enhanced performance for Cu(II) removal from water, J. Membr. Sci., 415 (2012) 250–259.

[11] M. Amini, M. Jahanshahi, A. Rahimpour, Synthesis of novel thin film nanocomposite (TFN) forward osmosis membranes using functionalized multi-walled carbon nanotubes, J. Membr. Sci., 435 (2013) 233–241.

[12] F.-F. Chang, W.-J. Liu, X.-M. Wang, Comparison of polyamide nanofiltration and low-pressure reverse osmosis membranes on As(III) rejection under various operational conditions, Desalination, 334 (2013) 10–16.

[13] M. Padaki, D. Emadzadeh, T. Masturra, A.F. Ismail, Antifouling properties of novel PSf and TNT composite membrane and study of effect of the flow direction on membrane washing. Desalination, 362 (2015) 141–150.

[14] S. Huang, M.-B. Wu, C.-Y. Zhu, M.-Q. Ma, J. Yang, J. Wu, Z.-K. Xu, Polyamide nanofiltration membranes incorporated with cellulose nanocrystals for enhanced water flux and chlorine resistance, ACS Sustainable Chem. Eng., 7 (2019) 12315–12322.

[15] M.F. Hamid, N. Abdullah, N. Yusof, N.M. Ismail, A.F. Ismail, W.N.W. Salleh, J. Jaafar, F. Aziz, W.J. Lau, Effects of surface charge of thin-film composite membrane on copper (II) ion removal by using nanofiltration and forward osmosis process, J. Water Process Eng., 33 (2020) 101032, doi: 10.1016/j.jwpe.2019.101032.

[16] V. Vatanpour, S.S. Madaeni, A.R. Khataee, E. Salehi, S. Zinadini, H. Ahmadi Monfared, TiO_2 embedded mixed matrix PES nanocomposite membranes: influence of different sizes and types of nanoparticles on antifouling and performance, Desalination, 292 (2012) 19–29.

[17] A. Adeniyi, D. Gonzalez-Ortiz, C. Pochat-Bohatier, O. Oyewo, B. Sithole, M. Onyango, Incorporation of Cellulose Nanocrystals (CNC) derived from sawdust into polyamide thin-film composite membranes for enhanced water recovery, Alexandria Eng. J., 59 (2020) 4201–4210.

[18] C. Xu, W. Chen, H. Gao, X. Xie, Y. Chen, Cellulose nanocrystal/silver (CNC/Ag) thin-film nanocomposite nanofiltration membranes with multifunctional properties, Environ. Sci.: Nano, 7 (2020) 803–816.

[19] F. Asempour, D. Emadzadeh, T. Matsuura, B. Kruczek, Synthesis and characterization of novel cellulose nanocrystals-based thin film nanocomposite membranes for reverse osmosis applications, Desalination, 439 (2018) 179–187.

[20] M. Jonoobi, A. Ashori, V. Siracusa, Characterization and properties of polyethersulfone/modified cellulose nanocrystals nanocomposite membranes, Polym. Test., 76 (2019) 333–339.

[21] A. Yao, Y. Yan, L. Tan, Y. Shi, M. Zhou, Y. Zhang, P. Zhu, S. Huang, Improvement of filtration and antifouling performance of cellulose acetate membrane reinforced by dopamine modified cellulose nanocrystals, J. Membr. Sci., 637 (2021) 119621, doi: 10.1016/j.memsci.2021.119621.

[22] Y. Liu, L. Bai, X. Zhu, D. Xu, G. Li, H. Liang, M.R. Wiesner, The role of carboxylated cellulose nanocrystals placement in the performance of thin-film composite (TFC) membrane, J. Membr. Sci., 617 (2021) 118581, doi: 10.1016/j.memsci.2020.118581.

[23] M. Ghanbari, D. Emadzadeh, W.J. Lau, T. Matsuura, M. Davoody, A.F. Ismail, Super hydrophilic TiO_2/HNT nanocomposites as a new approach for fabrication of high performance thin film nanocomposite membranes for FO application, Desalination, 371 (2015) 104–114.

[24] A. Rahimpour, M. Jahanshahi, A. Mollahosseini, B. Rajaeian, Structural and performance properties of UV-assisted TiO_2 deposited nano-composite PVDF/SPES membranes, Desalination, 285 (2015) 31–38.

[25] D. Emadzadeh, W.J. Lau, M. Rahbari-Sisakht, H. Ilbeygi, D. Rana, T. Matsuura, A.F. Ismail, Synthesis, modification and optimization of titanate nanotubes-polyamide thin film nanocomposite (TFN) membrane for forward osmosis (FO) application, Chem. Eng. J., 281 (2015) 243–251.

[26] F.A.A. Ali, J. Alam, A.K. Shukla, M. Alhoshan, B.M.A. Abdo, W.A. Al-Masry, A novel approach to optimize the fabrication conditions of thin-film composite RO membranes using multi-objective genetic algorithm II, Polymers, 12 (2020) 494., doi: 10.3390/polym12020494.

[27] C.Y. Tang, Y.-N. Kwon, J.O. Leckie, Effect of membrane chemistry and coating layer on physiochemical properties of thin-film composite polyamide RO and NF membranes: I. FTIR and XPS characterization of polyamide and coating layer chemistry, Desalination, 242 (2009) 149–167.

[28] H.M. Park, K.Y. Jee, Y.T. Lee, Preparation and characterization of a thin-film composite reverse osmosis membrane using a polysulfone membrane including metal-organic frameworks, J. Membr. Sci., 541 (2017) 510–518.

[29] H. Dong, L. Zhao, L. Zhang, H. Chen, C. Gao, W.S. Winston Ho, High-flux reverse osmosis membranes incorporated with NaY zeolite nanoparticles for brackish water desalination, J. Membr. Sci., 476 (2015) 373–383.

[30] Y. Ying, W. Ying, Q. Li, D. Meng, G. Ren, R. Yan, X. Peng, Recent advances of nanomaterial-based membrane for water purification, Appl. Mater. Today, 7 (2017) 144–158.

[31] L. Dambies, T.H. Vincent, E. Guibal, Treatment of arsenic-containing solutions using chitosan derivatives: uptake mechanism and sorption performances, J. Water Res., 36 (2020) 3699–3710.

[32] A. Seidel, J.J. Waypa, M. Elimelech, Role of charge (Donnan) exclusion in removal of arsenic from water by a negatively

charged porous nanofiltration membrane, Environ. Eng. Sci., 18 (2001) 105–113.
[33] Y. Sato, M. Kang, T. Kamei, Y. Magara, Performance of nanofiltration for arsenic removal, Water Res., 36 (2002) 3371–3377.
[34] S. Jiang, Y. Li, B.P. Ladewig, A review of reverse osmosis membrane fouling and control strategies, Sci. Total Environ., 595 (2017) 567–583.
[35] M. Morra, On the molecular basis of fouling resistance, J. Biomater. Sci., Polym. Ed., 11 (2000) 547–569.
[36] P. Daraei, N. Ghaemi, H. Sadeghi Ghari, An ultra-antifouling polyethersulfone membrane embedded with cellulose nanocrystals for improved dye and salt removal from water, Cellulose, 24 (2017) 915–929.
[37] Q. Cheng, Y. Zheng, S. Yu, H. Zhu, X. Peng, J. Liu, J. Liu, M. Liu, C. Gao, Surface modification of a commercial thin-film composite polyamide reverse osmosis membrane through graft polymerization of N-isopropylacrylamide followed by acrylic acid, J. Membr. Sci., 447 (2013) 236–245.
[38] Q. Luo, L. Cheng, M. Zhang, Y. Mao, Y. Hou, W. Qin, J. Dai, Y. Liu, Comparison and characterization of polyacrylonitrile, polyvinylidene fluoride, and polyvinyl chloride composites functionalized with ferric hydroxide for removing arsenic from water, Environ. Technol. Innovation, 24 (2021) 101927, doi: 10.1016/j.eti.2021.101927.
[39] Y.-M. Zheng, S.-W. Zou, K.G. Nadeeshani Nanayakkara, T. Matsuura, J. Paul Chen, Adsorptive removal of arsenic from aqueous solution by a PVDF/zirconia blend flat sheet membrane, J. Membr. Sci., 374 (2011) 1–11., doi: 10.1016/j.memsci.2011.02.034.
[40] A. Maghsodi, L. Adlnasab, In-situ chemical deposition as a new method for the preparation of Fe_3O_4 nanoparticles embedded on anodic aluminum oxide membrane (Fe_3O_4@AAO): characterization and application for arsenic removal using response surface methodology, J. Environ. Chem. Eng., 7 (2019) 103288, doi: 10.1016/j.jece.2019.103288.
[41] A.M. Nasir, P.S. Goh, A.F. Ismail, Highly adsorptive polysulfone/hydrous iron-nickel-manganese (PSF/HINM) nanocomposite hollow fiber membrane for synergistic arsenic removal, Sep. Purif. Technol., 213 (2019) 162–175.
[42] J. Ji, Y. Yun, Z. Zeng, R. Wang, X. Zheng, L. Deng, C. Li, Preparation and arsenic adsorption assessment of PPESK ultrafiltration membranes with organic/inorganic additives, Appl. Surf. Sci., 351 (2015) 715–724.
[43] C.M. Nguyen, S. Bang, J. Cho, K.-W. Kim, Performance and mechanism of arsenic removal from water by a nanofiltration membrane, Desalination, 245 (2009) 82–94.
[44] H. Saitúa, M. Campderrós, S. Cerutti, A.P. Padilla, Effect of operating conditions in removal of arsenic from water by nanofiltration membrane, Desalination, 172 (2005) 173–180.